IEEE Access
Multidisciplinary | Rapid Review | Open Access Journal

SPECIAL SECTION ON KEY ENABLING TECHNOLOGIES FOR PROSUMER ENERGY MANAGEMENT

Received January 6, 2021, accepted January 25, 2021, date of publication January 28, 2021, date of current version February 5, 2021.

Digital Object Identifier 10.1109/ACCESS.2021.3055223

Hybrid Measurements-Based Fast State Estimation for Power Distribution System

XI HE[1], (Member, IEEE), CHANG LI[2], (Member, IEEE), MINGDI DU[1], HENG DONG[1], AND PENG LI[3], (Senior Member, IEEE)

[1]Department of Electrical and Information Engineering, Hunan Institute of Technology, Hengyang 421002, China
[2]Center of Electrical Power and Energy, Department of Electrical Engineering, Technical University of Denmark, 2800 Kongens Lygnby, Denmark
[3]Digital Research Institute, China Southern Power Grid, Guangzhou 510663, China

Corresponding author: Xi He (forevermau@163.com)

This work was supported in part by the National Key Research and Development Program of China under Grant 2017YFB0902900; in part by the Provincial Educational Department Fund for Excellent Young Scholars under Grant 19B137; in part by the Hunan Education Department Project under Grant 18B468 and Grant 18C0899; and in part by the National College Students Innovative & Entrepreneurship Training Scheme under Grant S202011528005.

ABSTRACT The distribution grid is undergoing profound changes nowadays, and state estimator has become an essential part in the control room to enable future smart grid. The newly deployed micro phase measurement units (μPMU) and advanced metering infrastructure (AMI) devices make the real-time state estimation possible for distribution system. Therefore, this paper studies the incorporation and process of the multi-source measurements and proposes a fast three-phase state estimation based on the hybrid measurements scheme. By the process of μPMU measurements, pseudo voltage measurements are added, which significantly increases the estimation redundancy. For AMI measurements, the harmonic components model is used to overcome the asynchronicity problem. An improved sequential state estimation based on the changed measurements is proposed to enable a fast estimation. IEEE 13-node and 390-node systems are simulated to verify the efficacy and efficiency of the proposed method.

INDEX TERMS Advanced metering infrastructure (AMI), micro phase measurement units (μPMU), sequential state estimation, hybrid measurements scheme.

I. INTRODUCTION

Power system operating states can be classified into three possible scenarios, namely normal, emergency and restorative, as the operating conditions change. It is desirable to maintain the operating conditions in a normal and secure state. State estimation (SE) could be used for this purpose. Since the set of complex node voltages (or branch currents) can fully specify the system, they are often referred to as the static state of the system.

State estimation has been an essential part of the energy management system (EMS) in high-voltage level power transmission system for decades. However, this is not the case for distribution power system. There is a good reason for this lagging development in distribution grid: historically, there was no need to develop such capability given to the simplicity of distribution system. It only needs to estimate the operating condition, e.g., peak load or fault current, rather than continually monitor the actual operating state. Hence, the measurement instruments are quite few beyond the substations. But with the increasing integrated renewable resources, as well as the ever-growing scale of the distribution network, the need to better monitor, observe and understand the distribution gird is dramatically increasing [1]. Distribution system state estimation (DSSE) becomes the key enabler for "Active Distribution Network" (ADN), which including many applications, e.g., Volt/Var power management, overcurrent protection, demand response, distributed generation integration and dispatch, outage management, etc.

The two main obstacles for implementing state estimator nowadays in distribution grid are:

- Very few measurements are available, many of which are pseudo measurements with low accuracy.
- Lack of suitable method to deal with the ever-increasing smart meters, e.g., μPMU and AMI, due to the unique characteristic of these measurements. Let alone a proper approach for fast DSSE with the hybrid measurements.

The associate editor coordinating the review of this manuscript and approving it for publication was Bin Zhou.

There are other problems encountered compare to transmission SE, many of which are pointed out and addressed in the previous literature, e.g.

- Low X/R ratios and three-phase unbalances complicate the Jacobian matrix as well as the Gain matrix.
- The state of transformer/regulator taps, switches, and capacitor bank is not directly monitored, which jeopardizes the network observability.

This paper studies the design and implementation of a fast three phase DSSE, which makes the most use of the limited measurements in such context. The contributions of this paper can be summarized in three aspects:

1) The process and manipulation of the newly emerged measurements, i.e., the μPMU and AMI measurements, are studied. For the μPMU measurements, the pseudo voltage measurements as well as its standard deviation are presented, which improve the measurement redundancy in distribution system. Further, the incident current phasors are manipulated in rectangular coordinates in order to circumvent numerical problems. For AMI measurements, the short-term load estimation based on harmonic components model is used to overcome the asynchronicity problem.

2) An improved sequential DSSE based on changed measurements is proposed, which enables fast state estimation. The proposed algorithm is an extension of the original sequential SE proposed in [2]-[4]. By only processing the changed measurements during every execution, the estimation can be done very fast.

3) The proposed algorithm using hybrid measurements is verified by both IEEE test feeder and practical implementation.

This paper is structured as follows. Section II discusses the state-of-the-art and presents a brief literature review. Section III and Section IV provide the methodology of μPMU measurements and AMI measurements process. Section V presents the modified sequential SE algorithm. Section VI verifies the proposed approach by simulation. Section VII introduces the field implementation and concludes the paper.

II. STATE-OF-THE-ART

The state estimation technique was originally developed for aerospace. Based on his aerospace working experiences, Fred C. Schweppe adapted and extended it to meet the power system needs in 1970s [5]–[7]. The static model $Z = f(x_{ture}) + n$ and minimization function for state vectors estimation, i.e., $J(x) = [z - f(x)]'\theta^{-1}[z - f(x)]$ lay the foundation of static-state estimation. Further, an approximate model was proposed which not only simplifies the nonlinear equations to become linear but also divides the overall problem into two separate problems, i.e., the real power-voltage angles(P–δ) and the reactive power-voltage magnitude (Q–V) equalities. However, there are several preconditions for implementing this approximate model though, such as X/R $\gg$ 1, V$\approx$1 (all bused), and $\delta_i - \delta_k$(adjacent buses) $\approx$0, which are not so evident in distribution system.

Assuming the measurements errors have a known probability distribution with unknown parameters, a likelihood function can be obtained using the joint probability density function for all the measurements. Hence, an optimization function, namely the maximum likelihood function, can be set up to estimate the unknown parameters [8]. From this deduction, the weighted least square estimation is formed. Considering the different accuracy of each measurement, weighted least square (WLS) refines the primitive approach by adding the weights to each of the measurement. Thus, the objective function will be $J\big|_{X=\hat{X}} = \sum_{i=1}^{m} \frac{1}{\sigma_i^2} [Z_i - h_i(\hat{X})]^2 = min$.

In the 1990s, researchers dedicated more efforts to the area of DSSE. In the early days, there are very few measurements available to monitor the distribution network. Mesut E. Baran and Arthur W. Kelly innovatively proposed a branch-current-based three-phase DSSE instead of the conventional node-voltage-based DSSE [9]–[11]. The method enables decoupled Jacobian Matrix on a phase basis and is computationally efficient for radial and weakly meshed networks. After this novel method, successive efforts either dedicate to refine the original methodology or use it for other applications, e.g., topology processing [12], [13].

In recent years, lots of smart meters have been installed at the consumer side for billing and load monitoring purpose. For instance, a total of 59,940,150 meters have been installed by the end of 2019 in United States, and this accounts for 47% of the U.S. households [14]. In British Columbia, Canada, BC Hydro installed one million smart meters for nearly every consumer [15]. These AMI data should be very useful as a replacement for inaccurate pseudo-measurements. However, the asynchronicity problem caused by the different sampling times of the individual metering devices jeopardizes the complete snapshot of the network [16].

The angle phase differences in distribution grid are not measurable with the traditional PMU used in transmission grid because of the value is too small. Generally, in distribution system the voltage angle between two locations will be two orders smaller than those in transmission system (tenths of a degree rather than tens) [17]. First developed by Power Standards Lab (PSL) in Alameda, California, it has 0.001° resolution on voltage and current phase angles and 2 PPM resolution on voltage and current magnitudes. The reporting rate is t two times per cycle, i.e., 100/s at 50Hz or 120/s at 60Hz [18]. Despite its accuracy, high sample rating, and multi measurements, μPMU will not make DSSE obsolete but improve its performance together with the traditional monitoring system.

III. THE PROCESS OF PMU MEASUREMENTS

In distribution grid, the active and reactive power flows and power injections, as well as the voltage magnitudes are measured by distribution SCADA system, while the voltage phasors of the installed bus and current phasors of all the incident lines are measured by μPMU. The roll-out

of μPMU is still in its early stage (the pioneer project was conducted in 2014 at UC Berkley), and the device is rather expensive. It is uneconomical to implement the devices massively. Therefore, only the critical points, which means the network will become unobservable without any one of these points, are equipped with μPMU devices. The electric power distribution system for SE research purpose is usually defined as the part between the distribution substations and distribution transformers, including the several main transformers, many distribution transformers and low voltage buses in between.

To increase measurement redundancy, it is desirable to have some pseudo-measurements with comparatively high accuracy. Thus, in this paper, the bus voltage at the other end of the line (the line is connected to the bus where μPMU is installed) is calculated as pseudo-measurement.

A. INCREASE REDUNDANCY

Consider the three-phase line circuit as shown in Fig.1, which takes the magnetic coupling between different phases into account. Assuming μPMU installed at bus 1, the three-phase voltage phasor $\boldsymbol{V_1}$of bus 1 and the current phasor $\boldsymbol{I_{12}}$ of line 1-2are measured, denote as $\boldsymbol{V_1} = V_1\angle\delta_1$, $\boldsymbol{I_{12}} = I_{12}\angle\theta_{12}$ respectively. (In this paper, the variable in bold denotes phasor, otherwise scalar)

It is easy to have

$$\begin{bmatrix} \boldsymbol{V_{2.a}} \\ \boldsymbol{V_{2.b}} \\ \boldsymbol{V_{2.c}} \end{bmatrix} = \begin{bmatrix} \boldsymbol{V_{1.a}} \\ \boldsymbol{V_{1.b}} \\ \boldsymbol{V_{1.c}} \end{bmatrix} - \begin{bmatrix} z_{11} & z_{12} & z_{13} \\ z_{21} & z_{22} & z_{23} \\ z_{31} & z_{32} & z_{33} \end{bmatrix} \begin{bmatrix} \boldsymbol{I_{12.a}} \\ \boldsymbol{I_{12.b}} \\ \boldsymbol{I_{12.c}} \end{bmatrix} \tag{1}$$

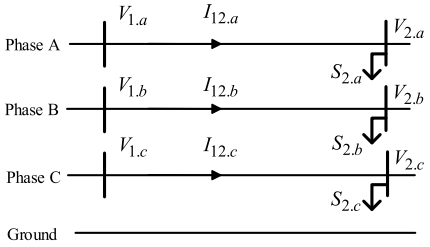

FIGURE 1. A three-phase line with μPMU measurements.

where matrix $\boldsymbol{z}$ represents the self and coupling impedance of different phases.

The pseudo-measurement $\boldsymbol{V_2}$ is obtained from (1). However, the standard deviation of $\boldsymbol{V_2}$ needs to be calculated to use it identical to the real measurements. In this paper, the classical uncertainty propagation theory is used to calculate the standard deviation of the pseudo-measurements [19], [20]. Consider phase A for illustration, rewrite $\boldsymbol{V_{2.a}}$ in the rectangular coordinates:

$$\boldsymbol{V_{2.a}} = V_{2.a}^r + jV_{2.a}^i \tag{2}$$

where the superscript "r" denotes the real parts of the vector and "i" denotes and imaginary parts. Thus we have

$$\begin{aligned} V_{2.a}^r = {} & V_{1.a}\cos\delta_{1.a} - r_{11}I_{12.a}\cos\theta_{12.a} + x_{11}I_{12.a}\sin\theta_{12.a} \\ & - r_{12}I_{12.b}\cos\theta_{12.b} + x_{12}I_{12.b}\sin\theta_{12.b} \\ & - r_{13}I_{12.c}\cos\theta_{12.c} + x_{13}I_{12.c}\sin\theta_{12.c} \end{aligned} \tag{3}$$

$$\begin{aligned} V_{2.a}^i = {} & V_{1.a}\sin\delta_{1.a} - r_{11}I_{12.a}\sin\theta_{12.a} - x_{11}I_{12.a}\cos\theta_{12.a} \\ & - r_{12}I_{12.b}\sin\theta_{12.b} - x_{12}I_{12.b}\cos\theta_{12.b} \\ & - r_{13}I_{12.c}\sin\theta_{12.c} - x_{13}I_{12.c}\cos\theta_{12.c} \end{aligned} \tag{4}$$

From (3) and (4), it is evident that the real part and imaginary part of the calculated voltage are functions of the voltage and current phasors measured by μPMU. Thus, V_2^r and V_2^i can be expressed as

$$V_{2.a}^r = f_{V_{2.a}^r}(V_{1.a}, \delta_{1.a}, I_{12.a}, \theta_{12.a}, I_{12.b}, \theta_{12.b}, I_{12.c}, \theta_{12.c}) \tag{5}$$

$$V_{2.a}^i = f_{V_{2.a}^i}(V_{1.a}, \delta_{1.a}, I_{12.a}, \theta_{12.a}, I_{12.b}, \theta_{12.b}, I_{12.c}, \theta_{12.c}) \tag{6}$$

According to the classical uncertainty propagation theory, the standard deviation of $\boldsymbol{V_2}$ can be expressed as follow [19]:

$$\sigma(V_2^r) = \sqrt{\sum_{k=1}^{4}[\partial V_2^r/\partial \boldsymbol{x}(k)]^2[\sigma(\boldsymbol{x}(k))]^2} \tag{7}$$

$$\sigma(V_2^i) = \sqrt{\sum_{k=1}^{4}[\partial V_2^i/\partial \boldsymbol{x}(k)]^2[\sigma(\boldsymbol{x}(k))]^2} \tag{8}$$

where $\boldsymbol{x} = [V_{1.a}, \delta_{1.a}, I_{12.a}, \theta_{12.a}, I_{12.b}, \theta_{12.b}, I_{12.c}, \theta_{12.c}]$, and $\sigma(\boldsymbol{x}(k))$ is the standard deviation of the μPMU measurements which are supposed to be known according to the instrument specification. The partial derivatives are computed in Table 1, where r, x are the line resistance and reactance respectively.

TABLE 1. Partial deviation of the pseudo voltage measurements.

$\frac{\partial V_{2.a}^r}{\partial V_{1.a}} = cos\delta_{1.a}$	$\frac{\partial V_{2.a}^r}{\partial \delta_{1.a}} = -V_{1.a}\sin\delta_{1.a}$
$\frac{\partial V_{2.a}^r}{\partial I_{12.a}} = -r_{11}\cos\theta_{12.a} + x_{11}\sin\theta_{12.a}$	$\frac{\partial V_{2.a}^r}{\partial \theta_{12.a}} = r_{11}I_{12.a}\sin\theta_{12.a} + x_{11}I_{12.a}\cos_{12.a}$
$\frac{\partial V_{2.a}^r}{\partial I_{12.b}} = -r_{12}\cos\theta_{12.b} + x_{12}\sin\theta_{12.b}$	$\frac{\partial V_{2.a}^r}{\partial \theta_{12.b}} = r_{12}I_{12.b}\sin\theta_{12.b} + x_{12}I_{12.b}\cos_{12.b}$
$\frac{\partial V_{2.a}^r}{\partial I_{12.c}} = -r_{13}\cos\theta_{12.c} + x_{13}\sin\theta_{12.c}$	$\frac{\partial V_{2.a}^r}{\partial \theta_{12.c}} = r_{13}I_{12.c}\sin\theta_{12.c} + x_{13}I_{12.c}\cos_{12.c}$
$\frac{\partial V_{2.a}^i}{\partial V_{1.a}} = sin\delta_{1.a}$	$\frac{\partial V_{2.a}^i}{\partial \delta_{1.a}} = V_{1.a}\cos\delta_{1.a}$
$\frac{\partial V_{2.a}^i}{\partial I_{12.a}} = -r_{11}\sin\theta_{12.a} - x_{11}\cos\theta_{12.a}$	$\frac{\partial V_{2.a}^i}{\partial \theta_{12.a}} = -r_{11}I_{12.a}\cos_{12.a} + x_{11}I_{12.a}\sin\theta_{12.a}$
$\frac{\partial V_{2.a}^i}{\partial I_{12.b}} = -r_{12}\sin\theta_{12.b} - x_{12}\cos\theta_{12.b}$	$\frac{\partial V_{2.a}^i}{\partial \theta_{12.b}} = -r_{12}I_{12.b}\cos\theta_{12.b} + x_{12}I_{12.b}\sin_{12.b}$
$\frac{\partial V_{2.a}^i}{\partial I_{12.c}} = -r_{13}\sin\theta_{12.c} - x_{13}\cos\theta_{12.c}$	$\frac{\partial V_{2.a}^i}{\partial \theta_{12.c}} = -r_{13}I_{12.c}\cos\theta_{12.c} + x_{13}I_{12.c}\sin_{12.c}$

It is worth pointing out that the reliability of the pseudo voltage measurements is relatively high due to the high accuracy of the μPMU measurements. In this way, the measurement redundancy is increased with very reliable data, which will boost the SE accuracy significantly.

B. CURRENT PHASOR MEASUREMENT

To include the current phasor measurements, the rectangular coordinates are used to calculate the Jacobian matrix in this paper. For most SE methods, the polar coordinates are used for computing measurement functions and Jacobian matrix, and the μPMU itself provides voltage and current phasors in the polar form. However, in distribution network where the shunt conductance and susceptance are normally negligible due to the short lines, the partial derivatives of the current measurements will be undefined (the denominator will be zero) if polar coordinates are used.

According to (1), the line current can be expressed as:

$$\boldsymbol{I_{12}} = (\boldsymbol{V_1} - \boldsymbol{V_2}) \cdot \boldsymbol{Y} \tag{9}$$

where $\boldsymbol{Y}$ is the admittance matrix. Chose phase A for analysis,

$$\begin{aligned}\boldsymbol{I_{12.a}} = {} & \boldsymbol{Y_{11}}(\boldsymbol{V_{1.a}} - \boldsymbol{V_{2.a}}) + \boldsymbol{Y_{12}}(\boldsymbol{V_{1.b}} - \boldsymbol{V_{2.b}}) \\ & + \boldsymbol{Y_{13}}(\boldsymbol{V_{1.c}} - \boldsymbol{V_{2.c}})\end{aligned} \tag{10}$$

The entries of Jacobian matrix relating to the current measurements can be expressed as:

$$\frac{\partial I^r_{12.a}}{\partial V_{1.a}} = g_{11}\cos\delta_{1.a} - b_{11}\sin\delta_{1.a} \tag{11}$$

$$\frac{\partial I^r_{12.a}}{\partial \delta_{1.a}} = -g_{11}V_{1.a}\sin\delta_{1.a} - b_{11}V_{1.a}\sin\delta_{1.a} \tag{12}$$

$$\frac{\partial I^i_{12.a}}{\partial V_{1.a}} = g_{11}\sin\delta_{1.a} + b_{11}\cos\delta_{1.a} \tag{13}$$

$$\frac{\partial I^i_{12.a}}{\partial \delta_{1.a}} = g_{11}V_{1.a}\cos\delta_{1.a} - b_{11}V_{1.a}\sin\delta_{1.a} \tag{14}$$

where I^r_{12} and I^i_{12} represent the real and imaginary parts of $\boldsymbol{I_{12}}$ respectively.

It is evident that the numerical problem can be circumvented when use the rectangular coordinates for current measurements, and the partial deviates are more concise when put state vectors in rectangular form [21]. It is worth noting that the state vectors are still in polar form because it would be easier for power flow, power injection, and voltage magnitude manipulation.

In this paper, the traditional voltage magnitude and angle are chosen as state vectors, while the measurements are expressed in rectangular coordinates forms.

IV. THE PROCESS OF AMI MEASUREMENTS

The early DSSE tend to use the statistical load data to overcome low measurement redundancy problem. However, the historical measurements or estimated load data are rather inaccurate, e.g., the variation of the pseudo measurements is assumed to be 20%,30%, and 50% in [22]–[24], respectively. With such imprecise data, the result would be compromised inevitably. With the proliferation of smart metering devices, the active and reactive power injection is available now at the consumer end. The consumer side meters are originally used for billing purpose with 15- or 30-mins sampling intervals. In previous literature, such as [25], [26], the authors recognized that there is a significant delay in AMI data due to the low report rate. In this paper, we allow 2 mins delay between the data being sampled in the field and received by the control room. This amount of delay is testified in the practical implementation as we consider the transmission time.

Due to the power loss from the low-voltage distribution transformer to the consumers are relatively small (very short lines), the transformer's load is simply the summation of the data collected by the AMI meters at a certain time. As shown in Fig. 2, each of the nodes (LV transformer) is seen as the start point of the low-voltage network, which includes about 100-150 households normally in the urban distribution network. The active and reactive power of the transformer I at time t can be expressed as follows:

$$P^i_t \doteq \sum_{n=1}^{N} p^i_{t,n} \tag{15}$$

$$Q^i_t \doteq \sum_{n=1}^{N} q^i_{t,n} \tag{16}$$

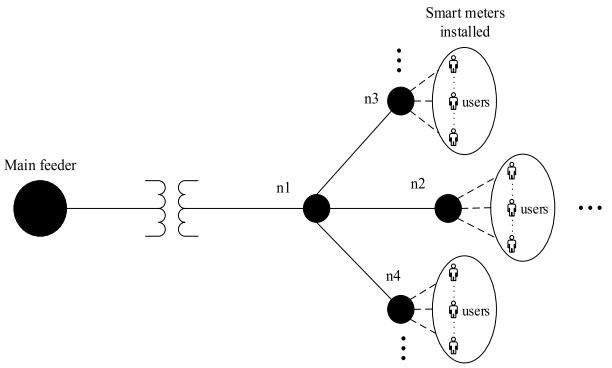

FIGURE 2. A simplified MV network.

However, the smart meters do not transmit the data all at the same time due to the bandwidth limitation. As illustrated in Fig. 3, the sampling and update interval are both 15 mins, while there is approximate 2 mins delay between the two. Each of the meters may have its own sampling instant. We assume that a distribution transformer (DT) contains three consumers, i.e., Meter 1, Meter 2, and Meter 3 as shown in Fig. 3. If we want to know the power injection at time 2, Meter 1, Meter 2, and Meter 3 can only provide the measurements which are sampled at time 0, −14, and −11 respectively. Therefore, a snapshot of the entire network is not possible due to the asynchronized sampling instant.

Consider that it is a short-term load forecast here (less than 16 min), and the load variation can be seen as a distorted sinusoid, the harmonic components model that expressed in Fourier series is used to represent the load variation [27]. The

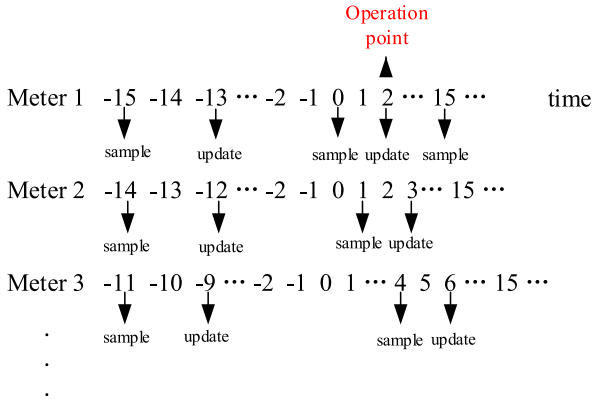

FIGURE 3. The time series of AMI sampling & update procedure.

short-term load forecast can be denoted as follow:

$$l(t) = l'(last) + \sum_{n=1}^{N}\left[a_n \cos(\frac{2\pi nt}{96}) + b_n \sin(\frac{2\pi nt}{96})\right] \quad (17)$$

where $l'(last)$ denotes the last update load value and the second part denotes the load variation from the last sampling to the time where state estimation is performed. The denominator is 96 because there are 96 samples per day (a daily circle), and N is the orders of the harmonic components. Here, different orders of harmonics are used for different meters accordingly.

Still consider Fig. 3 and the example illustrated in the last paragraph. We assume DSSE is performed at time 2 (the operation point). For Meter 1, Meter 2, and Meter 3, the interval between the last sampling (LS) and the operation point (OP) is 2, 16, and 13, respectively. It is found that the maximum order of the harmonics is 5 in order to keep calculation efficiency [28]. Table 2 shows the harmonic orders used for different LS& OP intervals. Hence, for Meter 1, Meter 2, and Meter 3, the load forecast in time 2 can be presented as:

$$meter1 : l(2) = l'(2) + a_1 \cos(\frac{\pi}{48}) + b_1 \sin(\frac{\pi}{48}) \quad (18)$$

$$meter2 : l(2) = l'(-12) + \sum_{n=1}^{5}\left[a_n \cos(\frac{\pi n}{48}) + b_n \sin(\frac{\pi n}{48})\right] \quad (19)$$

$$meter3 : l(2) = l'(-9) + \sum_{n=1}^{4}\left[a_n \cos(\frac{\pi n}{48}) + b_n \sin(\frac{\pi n}{48})\right] \quad (20)$$

Note that in (19) and (20), we set $t = 1$ in the *sine* and *cosine* function because that the next update time is near the operation point ($t = 2$). The moment $t = 0$ is assumed as the beginning of the day. Parameters a_n and b_n are the unknown, which need to be calculate from the historical data.

In [28], the authors use Anderson-Darling and Shapiro-Wilk tests to prove that the load variation of the "outdated signal" is normally distributed. It means that the error of the outdated signal can be modeled as random variables, which also related to the LS and OP intervals. Also, we assume the standard deviation varies linearly in the interval. Thus the standard deviation at the operation point is calculated as:

$$\sigma(op) = \sqrt{\sigma^2(last) + \frac{IN_{length}}{16}\left(\sigma^2(last) - \sigma^2(last-1)\right)} \quad (21)$$

where $\sigma^2(last)$ and $\sigma^2(last-1)$ are the variance of the latest update and the second latest update, respectively. IN_{length} denotes the length of the interval.

TABLE 2. The harmonic orders of different intervals.

LS&OP Intervals	2-4	5-7	8-10	11-13	14-16
Harmonic Orders	1	2	3	4	5

V. PROPOSED STATE ESTIMATION METHOD

Under normal operation, only a small portion of the measurements have changed its value compare to the time of the previous estimation performance. Compare to the unchanged measurements, the changed measurements dominate the variation of state vectors. Based on the method explained above, we proposed an approach that only processes the changed measurements sequentially to conduct the state estimation. The possibility of only employing truncated measurements is that a good number of redundant measurements exist. If the measurements redundancy is rather low, e.g., the redundancy is 1(which means the network is merely observable), the unchanged or barely changed measurements can't be omitted. The necessity of deploying truncated measurements is that the estimation is conducted very frequently, and the measurements are updated very fast. With such a short estimation performance interval, a good portion of measurements will maintain unchanged or barely changed. The use of only changed measurements rather than the whole measurements will undoubtedly accelerate the estimation performance.

In a definite network with known parameters and topology, the nonlinear measurement function can be denoted as

$$\boldsymbol{z} = \boldsymbol{h}(\boldsymbol{x}) + \boldsymbol{v} \quad (22)$$

Using WLS algorithm, the objective function is

$$\boldsymbol{J}(x) = [\boldsymbol{z} - \boldsymbol{h}(x)]^T \boldsymbol{R}^{-1}[\boldsymbol{z} - \boldsymbol{h}(x)] \quad (23)$$

The state vector $\boldsymbol{x}$, which enables the least $\boldsymbol{J}(x)$ are defined as the optimal estimated state variable, denoted as $\hat{\boldsymbol{x}}$. In (23), $\boldsymbol{z}$ is the measurements matrix, $\boldsymbol{h}(x)$ is the measurement function, and $\boldsymbol{R}^{-1}$ is the diagonal matrix with elements of measurements weight, which is the reciprocal of the measurement variance.

During two consecutive estimations, the measurements matrix is changed $\Delta\boldsymbol{z}$.The sensitivity relation of state variable change and measurement change, i.e., $\Delta\boldsymbol{x}$ and $\Delta\boldsymbol{z}$, is analyzed. First, we use the truncated Taylor series to linearize $\boldsymbol{h}(x)$ in the vicinity of x_0, which can be expressed as

$$\boldsymbol{h}(x) \approx \boldsymbol{h}(x_0) + \boldsymbol{H}(x_0)\Delta\boldsymbol{x} \quad (24)$$

where $\Delta \boldsymbol{x} = \boldsymbol{x} - \boldsymbol{x}_0$.

$$\boldsymbol{H}(x_0) = \left.\frac{\partial \boldsymbol{h}(x)}{\partial x}\right|_{x=x_0} \tag{25}$$

$\boldsymbol{H}(x)$ is a m^*n Jacobian matrix. Substituting (25) into (24), the objective function is formulated as

$$\boldsymbol{J}(x) = [\Delta \boldsymbol{z} - \boldsymbol{H}(x_0)\Delta \boldsymbol{x}]^T \boldsymbol{R}^{-1}[\Delta \boldsymbol{z} - \boldsymbol{H}(x_0)\Delta \boldsymbol{x}] \tag{26}$$

where $\Delta z = z - \boldsymbol{h}(x_0)$. Unfolding and manipulating (26), the objective function is equivalent to

$$\begin{aligned}\boldsymbol{J}(x) = {} & \Delta z^T[\boldsymbol{R}^{-1} - \boldsymbol{R}^{-1}\boldsymbol{H}(x_0)\boldsymbol{\Sigma}(x_0)\boldsymbol{H}^T(x_0)\boldsymbol{R}^{-1}]\Delta z \\ & + \left[\Delta \boldsymbol{x} - \boldsymbol{\Sigma}(x_0)\boldsymbol{H}^T(x_0)\boldsymbol{R}^{-1}\Delta z\right]^T \boldsymbol{\Sigma}^{-1}(x_0)[\Delta \boldsymbol{x} \\ & - \boldsymbol{\Sigma}(x_0)\boldsymbol{H}^T(x_0)\boldsymbol{R}^{-1}\Delta z]\end{aligned} \tag{27}$$

where $\boldsymbol{\Sigma}(x_0) = [\boldsymbol{H}^T(x_0)\boldsymbol{R}^{-1}\boldsymbol{H}(x_0)]^{-1}$. From (27), the first part of the equation is irrelevant to $\Delta \boldsymbol{x}$. In order to obtain the minimum $\boldsymbol{J}(x)$, the second part should be 0. Hence,

$$\Delta \boldsymbol{x} = \boldsymbol{\Sigma}(x_0)\boldsymbol{H}^T(x_0)\boldsymbol{R}^{-1}\Delta z \tag{28}$$

Thus, the sensitivity relationship between $\Delta \boldsymbol{x}$ and Δz at x_0 can be denoted by the sensitivity matrix ($m \times n$) as below,

$$\boldsymbol{S}_{x_0} = \frac{\Delta \boldsymbol{x}}{\Delta z} = \boldsymbol{\Sigma}(x_0)\boldsymbol{H}^T(x_0)\boldsymbol{R}^{-1} \tag{29}$$

The sensitivity of the state vectors to one measurement z_i at x_0 is $\boldsymbol{S}_{x_0,i}$, a column of $\boldsymbol{S}$ correspond to z_i. Assuming that $z_1, z_2, \cdots z_m$ are the changed measurement since the previous estimation performance, the measurement function is written as $z_m = \boldsymbol{h}(x_m) + \boldsymbol{v}_m$.

In the proposed estimation approach, a WLS estimator is required to start the performance using all the measurements available. From which, the initial state $\hat{x}_0$, sensitivity matrix $\boldsymbol{S}_{x_0}$ are obtained. Due to the real x_0 is unknown, $\hat{x}_0$ is used for solving the sensitivity matrix.

$$\begin{cases} \hat{\boldsymbol{x}}_m = \hat{\boldsymbol{x}}_{m-1} + \boldsymbol{S}_{\hat{x},m} \cdot \Delta z_m \\ \boldsymbol{S}_{\hat{x}} = \boldsymbol{\Sigma}(\hat{\boldsymbol{x}})\boldsymbol{H}^T(\hat{\boldsymbol{x}})\boldsymbol{R}^{-1} \\ \boldsymbol{P}_m = Diag\{[\boldsymbol{I} - \boldsymbol{k}_m\boldsymbol{H}_m(\hat{\boldsymbol{x}}_m)]\boldsymbol{P}_{m-1}\} \\ \boldsymbol{k}_m = \dfrac{\boldsymbol{P}_{m-1}\boldsymbol{H}_m^T(\hat{\boldsymbol{x}}_{m-1})}{\tau_m\sigma_m^2 + \boldsymbol{H}_m(\hat{\boldsymbol{x}}_{m-1})\boldsymbol{P}_{m-1}\boldsymbol{H}_m^T(\hat{\boldsymbol{x}}_{m-1})} \end{cases} \tag{30}$$

The equation set for the proposed sequential state estimation based on changed measurements for distribution gird are as (30), where $\boldsymbol{H}_m$ is the m_{th} row vector of the measurement Jacobian matrix; $\boldsymbol{P}_m$ is the error covariance matrix after the process of m_{th} changed measurement; *Diag* denotes the diagonal elements of the matrix; $\boldsymbol{k}_{\text{m}}$ is coefficient of the error covariance; σ_m^2 is the variance of the m_{th} measurement and τ_m is the tuning parameter used to compensate the omitted non-diagonal elements in error covariance. The empirical value of the tuning parameter range between 0.1∼1.0 [4].

It is worth noting that the sensitivity matrix does not have to calculate during every sequential process. The calculation frequency depends on the accumulation of the errors. If some emergencies happen, e.g., sudden heavy loads change, fault, topology changes, the sensitivity matrix should be calculated immediately. Another issue is the threshold value, which determines how much change of the measurement value can be regarded as ''changed measurement''. This is an engineering problem, because it depends on the process ability of the hardware and the accuracy requirement of the system. The basic principle is that it should be neither too large nor too small, and different types of measurements should employ different threshold values.

VI. CASE STUDIES

The proposed hybrid measurements based fast state estimation was implemented in Matlab R2019a and has been tested on IEEE 13- and 390-node test system. The reason why we chose these two test systems is that the IEEE 13-node test feeder is a very small test system and yet displays some very interesting characteristics, such as unbalanced spot and distributed loads, in-line transformer, etc. While the 390-node test system is a medium size benchmark featured with unbalanced heavily meshed low voltage networks. The majority of end-use customers in North America are served by radially operated distribution feeders. But in areas where there is a high load density and a need for very high reliability, Low Voltage Network (LVN) systems have been built. The 390-node test system is a Low Voltage Network Test System (LVNTS) that is fundamentally different in design and operation from typical radial distribution feeders, such as the 13-node test feeder. All the following simulations are executed on a computer with Intel Core i7 4.2 GHz, 16 GB of RAM and Windows 7 Ultimate Edition 64-bit operation system.

A. IEEE 13-NODE TEST SYSTEM

The one-line diagram of the IEEE 13 node test feeder is shown in Fig. 4, and the complete data for this system can be found in [29]. This feeder displays some very interesting characteristics, such as: a). Short and relatively highly loaded for a 4.16kV feeder; b). In-line transformer; c). Unbalanced spot and distributed loads; d). Overhead and underground lines with variety of phasing; e). One substation voltage regulator consisting of three single-phase units connected in wye. Therefore, this feeder provides a good test for the most common features of distribution analysis software.

The location of the μPMU is based on the Optimal PMU Placement (OPP) algorithm introduced in [30], which is suitable for radial distribution network. AMI meters are supposed to be installed at every load point, which is not specified in the figure. Table 3 illustrates the location of the meters and redundancy. For μPMU measurements, there are additional 7 voltage pseudo voltage measurements calculated through the direct measurements as we elaborated in Section III. In the simulation, the power loss of the lines is not considered.

The three-phase power flow simulator is used to generate the measurements with addition of normally distributed noise. Table 4 presents the accuracy of the three types of metering devices.

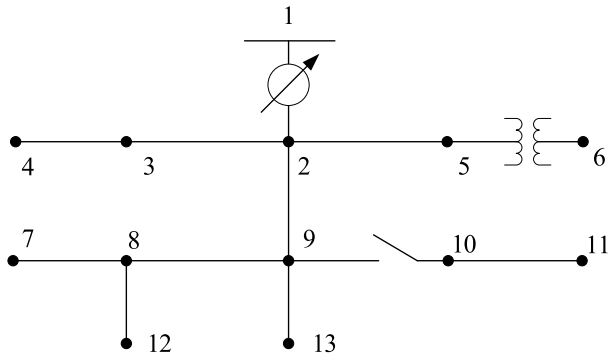

FIGURE 4. IEEE 13-bus distribution system.

TABLE 3. The measurement configuration for simulation system.

Type of the Meters	Placement	Number of the Measurements
SCADA	0	0
μPMU	2, 8, 9	16(direct measurements)
AMI	all the load points	12
Total State Variables: 24	Total Measurements:45	Redundancy: 1.17

TABLE 4. The measurement accuracy (deviation).

Type	Voltage/Current Magnitude	Phase Angle	Power
μPMU	0.2%	0.05	-
SCADA	2%	-	3%
AMI	-	-	0.5%

According to the proposed methods, we first calculate the pseudo voltage measurements, and it renders 7 additional measurements. It is worth noting that the classical uncertainty propagation theory is deployed to determine the calculation radius of the pseudo measurements. Otherwise, this process can be non-stop with undesirable values. For the AMI measurements, the proposed approach mainly deals with the time delay between the sampling time and receiving time. To evaluate the efficacy of the proposed method, we compare the proposed approach with two other distribution system state estimation methods, i.e., a generalized state estimation incorporated of Synchronized Phasor Measurements (GSE-PM) proposed in [31], and a practical multi-phase distribution state estimation solution incorporating smart meter and sensor data proposed in [25]. The former one takes the phasor measurements into consider, while the latter one takes care of the AMI data. Here, we abbreviate our hybrid measurements based method as HMBF-SE.

Fig. 5 is the voltage magnitude comparison of node 4 between the three different methods. Fig. 5(a) shows a sharp voltage surge during a sudden load decrease at node 4. From comparison, it can be seen that the proposed the HMBF-SE has a better following performance during load drop. Fig. 5(b) shows a sharp voltage dip during a sudden load increase at node 4. From the comparison, it can be seen that the curve of the proposed HMBF-SE is very similar to the true value, while the other two methods have a bigger deviation.

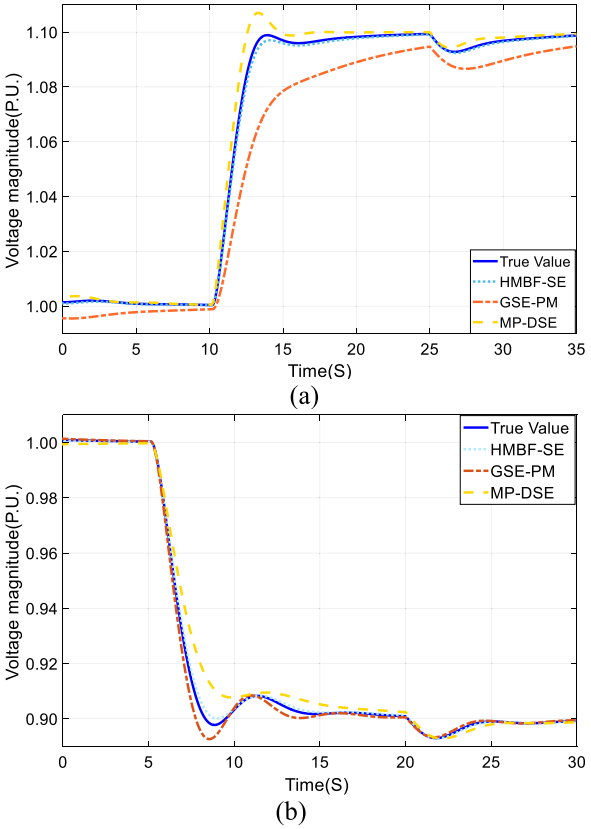

FIGURE 5. Voltage magnitude comparison between the proposed HMBF-SE and the GSE-PM proposed in [31], and MP-DSE proposed in [25]. (a) sharp load decrease at 10s. (b) sharp load increase at 5s.

Fig. 6 is the voltage angle comparison of node 4 between the three different methods. Fig. 6(a) and Fig. 6(b) show a voltage angle fluctuation during a sharp load variation. It is clear that the proposed method, i.e., HMBF-SE can best reflect the angle variation, while the GSE-PM and MP-DSE either has a lower angle estimation or a higher angle estimation. Even after the load fluctuation, the angle estimation of GSE-PM and MP-DSE remain inaccurate because of their inadequate process of phasor measurements or the AMI data.

B. IEEE 390-NODE TEST SYSTEM

The majority of end-use customers in North America are served by radially operated distribution feeders. But in areas where there is a high load density and a need for very high reliability, Low Voltage Network (LVN) systems have been built. LVNs are fundamentally different in design and operation from typical radial distribution feeders, and these differences require different methods for computational analysis. The LVNTS has been designed to present challenges to distribution system analysis software in the following areas: a)Heavily meshed and networked systems; b) Systems with

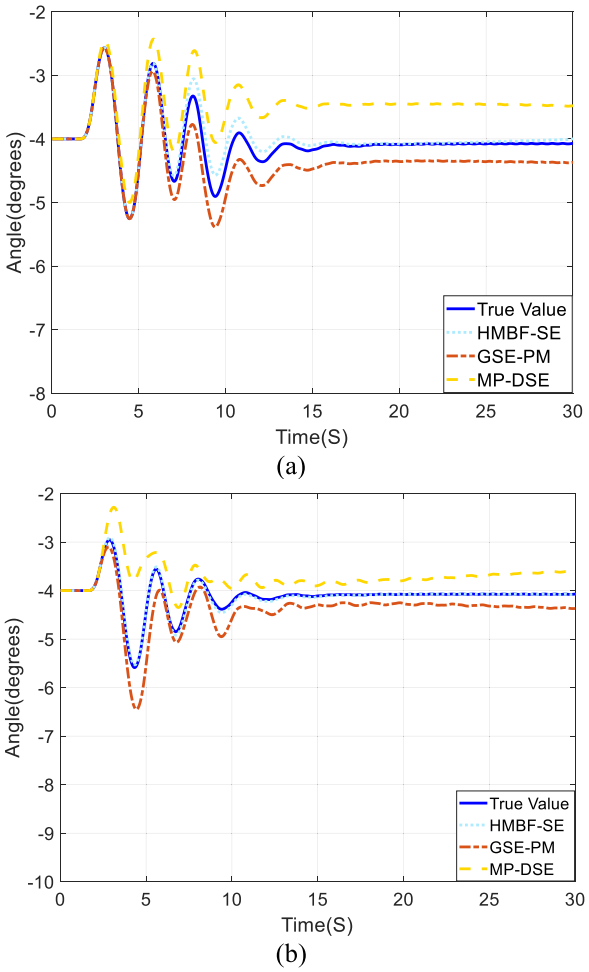

FIGURE 6. Voltage angle comparison between the proposed HMBF-SE and the GSE-PM proposed in [31], and MP-DSE proposed in [25]. (a) sharp load decrease at 2s. (b) sharp load increase at 2s.

numerous parallel transformers; c) Modeling of parallel low voltage cables.

The IEEE 390 node low voltage system is representative of low voltage network systems that are deployed in urban cores in North America. The power system in an urban core can be a combination of spot networks and grid networks. The LVNTS is composed of a single 120/208 V grid system and 8 277/480 V spot networks, all are wye-grounded. The grid system and spot networks are supplied by 8 13.2 kV distribution feeders supplied from a single substation, all are delta connected. Appendix A shows the one-line diagram of the entire LVNTS, with node numbers included. Primary voltages are shown in red and secondary voltages are shown in blue. Because of the complexity of the LVNTS, Figure 1 will be expanded into three separate figures; the primary distribution feeders, the grid network, and the 8 spot networks.

Due to the heavily meshed and networked characteristic of the 390 node LVN, the placement of the μPMU is determined based on the algorithm proposed in [32], rather than the algorithm used in the aforementioned 13 node test system. The specific meter placement is omitted here for simplicity and the measurement accuracy is the same as Table 4. Then we still compare the voltage magnitude angle estimation of the proposed method with the methods proposed in [25] and [31].

Fig. 7 is the voltage magnitude comparison of node 93 between the three different methods. From Fig. 7, the performance of the proposed method is better than the other two methods in the heavily meshed network during sharp load variation.

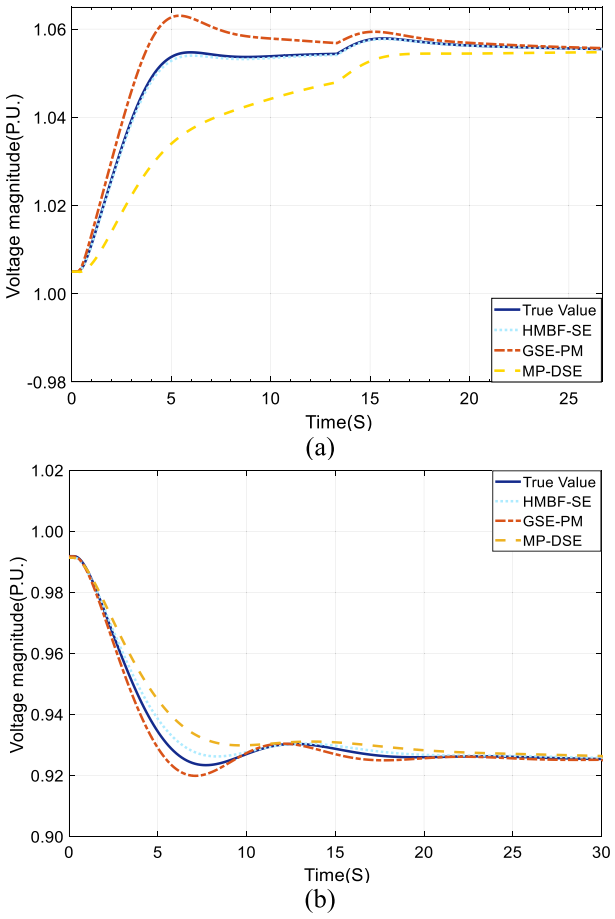

FIGURE 7. Voltage magnitude comparison between the proposed HMBF-SE and the GSE-PM proposed in [31], and MP-DSE proposed in [25]. (a) sharp load decrease at 0s. (b) sharp load increase at 0s.

Fig. 8 is the voltage angle comparison of node 93 between the three different methods. During sudden load increase or decrease, the angle will oscillate for several seconds. After the oscillation, the true voltage angle will deviate from the original one because we do not consider any regulation measures here.

C. THE EFFICIENCY OF THE PROPOSED METHOD

To verify the efficiency of the proposed method, which only tackles the changed measurements during every

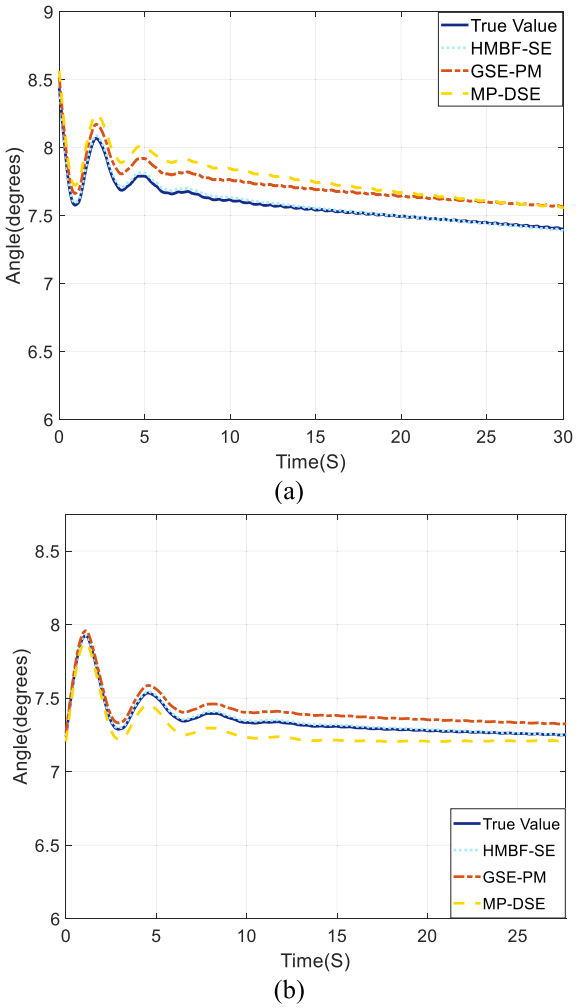

FIGURE 8. Voltage angle comparison between the proposed HMBF-SE and the GSE-PM proposed in [31], and MP-DSE proposed in [25]. (a) sharp load decrease at 0s. (b) sharp load increase at 0s.

iteration, we observe the whole iteration process of the state estimation. Here we deploy the IEEE 390 test system to conduct this simulation. Firstly, a full WLS algorithm using all the measurements is conducted to start the estimation. Thus the initial state and sensitivity matrix is obtained. For the first iteration, there are 332 changed measurements, including all the six types of measurements metered by SCADA, AMI and μPMU. It must point out that the changed measurements are randomly chosen and preset manually. The changed measurements account for roughly 20% of the total measurements and the threshold value is set to 1% for the voltage (current) magnitude, 5% for the power flow and load variation, 0.01° for the voltage (current) angle. The result of certain state variables after 16 iterations is shown in Table 5. From Table 5, it can be seen that the algorithm converges after 16 iterations and all 6 state variables reach a very high estimation accuracy. The convergence criteria $\xi = 4.16 \times 10^{-5}$. For all the 752 state variables, the statistic estimation error is calculated

TABLE 5. The evolution of four chosen state variables (l = 1 ∼ 16).voltage: p.u., angle: degree.

Iteration	V_{56}	δ_{56}	V_{308}	δ_{308}	$J(\hat{x})$
1	1.3457	-2.56	0.7665	112.43	102321.89
2	1.3032	-5.32	0.8143	119.43	6843.32
3	1.2654	-7.32	0.8501	125.42	2323.12
4	1.2332	-9.65	0.8954	129.09	879.09
5	1.2056	-10.11	0.9132	132.99	653.09
6	1.1821	-11.43	0.9254	134.54	321.58
7	1.1643	-12.76	0.9332	135.09	300.51
8	1.1456	-13.12	0.9454	136.33	289.48
9	1.1321	-13.34	0.9567	137.89	276.63
10	1.1265	-13.36	0.9611	137.99	266.77
11	1.1112	-13.44	09701	138.01	251.70
12	1.0989	-13.44	0.9765	138.02	248.01
13	1.0872	-13.43	0.9777	138.01	247.43
14	1.0721	-13.43	0.9781	138.02	246.62
15	1.0719	-13.44	0.9779	138.01	244.43
16	1.0721	-13.44	0.9779	138.02	244.43
True value	1.0721	-13.44	0.9780	138.00	238

by the following equations:

$$\bar{S}_M = \frac{1}{T}\sum_{t=1}^{T}\left[\frac{1}{m}\sum_{i=1}^{m}\left(\frac{z_{i,t}-S_{i,t}}{\sigma_i}\right)^2\right]^{\frac{1}{2}} \tag{31}$$

$$\bar{S}_E = \frac{1}{T}\sum_{t=1}^{T}\left[\frac{1}{m}\sum_{i=1}^{m}\left(\frac{h_{i,t}(\hat{x})-S_{i,t}}{\sigma_i}\right)^2\right]^{\frac{1}{2}} \tag{32}$$

where $z_{i,t}$, $h_{i,t}(\hat{x})$, $S_{i,t}$ are the measurement value, estimated value, and true value for one estimation, respectively. For a normal measurement system $\bar{S}_M \approx 1$. It is calculated that $\bar{S}_E = 0.66$, thus $\bar{S}_E/\bar{S}_M = 0.66 < 1$. It is evident that the proposed approach could estimate not only the unmetered variables but also enhance the measurement accuracy. The objective function $J(\hat{x})$ is supposed to be m-n if the estimation is optimal, where m is the total measurements number and n is the total state variables. From Table 5, it can be seen that $J(\hat{x}) = 244 \approx m - n$.

The actual CPU executing time is examined and compared for three different approaches, i.e., the proposed method, WLS and weighted least absolute value (WLAV). Each of the eight different distribution test feeders, i.e., 13, 34, 37, 123, 390, 800, and 1500, are simulated 10 times using the three different estimation algorithms. Table 6 shows that for small scale distribution systems, the CPU time spent by the three algorithms respectively are roughly identical. However, as the system is scaling up, the proposed approach which

TABLE 6. The CPU executive time comparison (unit: seconds).

Algorithm	34-node system	37-node system	390-node system	800-node system	1500-node system
HMBF-SE	0.13	0.13	6.32	10.82	15.32
WLS	2.34	2.54	16.13	24.34	43.22
WLAV	2.36	2.57	19.32	33.65	66.80

only uses the changed measurements to conduct SE saves a lot of time. For instance, the simulation time of the proposed method, WLS and WLAV algorithm for 390-node test feeder is 9.32, 16.13, 19.32 sec. respectively. For the 800-node system, the CPU time cost by the proposed method is only 50% of that cost by WLS.

VII. DISCUSSION AND CONCLUSION

A. DISCUSSION

The test version of the proposed method is implementing in one district of Guangzhou, a southern city of China. This pilot project covers 20 square kilometers, including three 110kV to 10 kV substations and twenty-two 10 kV feeders. In this project, 100 μPMUs and nearly 600 AMIs have be installed. In the confined trial district, the estimation accuracy, consistency, and speed of the estimator are overall satisfying.

There are some shortcomings of the proposed method which need to be improved in the future. One is the limited ability to deal with the three-phase unbalance. It is found that the estimation accuracy will be jeopardized if the three-phase unbalance of the feeder is more than 2%. Another concern is the performance consistency as the growing integration of distributed photovoltaic generation. The renewable energy integration will change the network topology profoundly and aggravate the three-phase unbalance problem. Another important issue regarding robust SE is bad data detection and identification, which is not discussed in this paper. Sequential state estimation itself has the advantage of dealing with leverage point and bad data. Nevertheless, it is worth improving the bad data processing mechanism since the data quality will be descending as the aging of the metering and transmission system.

B. CONCLUSION

This paper proposed an improved sequential SE algorithm base on multi-source measurements, which makes the most use of the newly installed meters and the legacy monitoring system. The hybrid measurements structure improves the measurement redundancy and the manipulation of the extremely accurate μPMU data adds additional pseudo-measurements which further raise redundancy. All the measurements are manipulated in rectangular coordinates in order to avoid numerical problem. The harmonic components model is used to forecast the extremely short-term load estimation, in this way, a snapshot of the entire network is obtained.

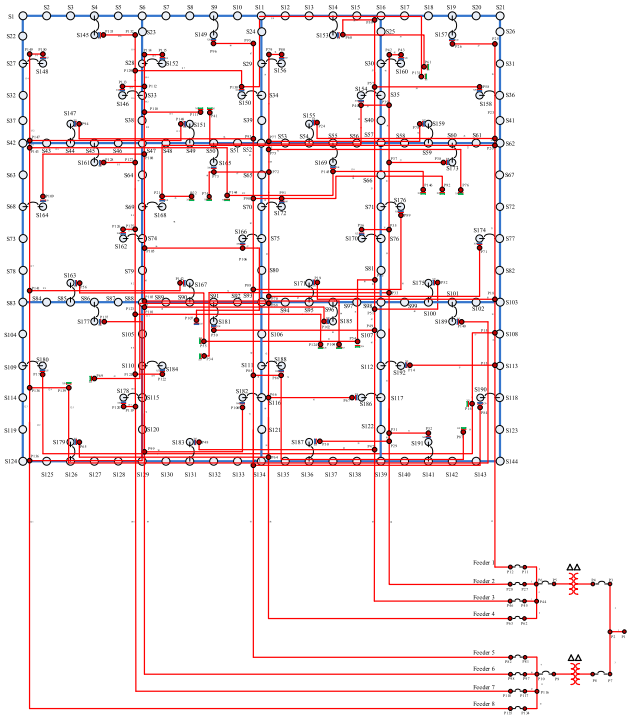

FIGURE 9. The one-line diagram of the entire LVNTS.

The simulation verifies the proposed estimation approach from four aspects: feasibility, accuracy, and efficiency. Some conclusions can be drawn from the test results: 1) the proposed manipulation of the μPMU and AMI data is effective to avoid numerical problems while obtaining a consistent snapshot of the entire network; 2) the additional pseudo voltage measurements boost estimation accuracy; 3) the proposed approach based on changed measurements can deal with massive and highly frequent data.

Through field implementation, some shortcomings of the proposed approach are exposed, which signposts the path for our future work.

APPENDIX A

See Fig 9.

REFERENCES

[1] A. V. Meier, D. Culler, A. McEachern, and R. Arghandeh, "Micro-synchrophasors for distribution systems," in *Proc. Innov. Smart Grid Technol. Conf.*, Washington, DC, USA, Feb. 2014, pp. 1–5.

[2] R. E. Larson, W. F. Tinney, and J. Peschon, "State estimation in power systems part I: Theory and feasibility," *IEEE Trans. Power App. Syst.*, vol. PAS-89, no. 3, pp. 345–352, Mar. 1970.

[3] R. E. Larson, W. F. Tinney, L. P. Hajdu, and D. S. Piercy, "State estimation in power systems part II: Implementation and applications," *IEEE Trans. Power App. Syst.*, vol. PAS-89, no. 3, pp. 353–363, Mar. 1970.

[4] A. Debs and R. Larson, "A dynamic estimator for tracking the state of a power system," *IEEE Trans. Power App. Syst.*, vol. PAS-89, no. 7, pp. 1670–1678, Sep. 1970.

[5] F. Schweppe and J. Wildes, "Power system static-state estimation, part I: Exact model," *IEEE Trans. Power App. Syst.*, vol. PAS-89, no. 1, pp. 120–125, Jan. 1970.

[6] F. Schweppe and D. Rom, "Power system static-state estimation, part II: Approximate model," *IEEE Trans. Power App. Syst.*, vol. PAS-89, no. 1, pp. 125–130, Jan. 1970.
[7] F. Schweppe, "Power system static-state estimation, part III: Implementation," *IEEE Trans. Power App. Syst.*, vol. PAS-89, no. 1, pp. 130–135, Jan. 1970.
[8] A. Abur and A. G. Exposito, *Power System State Estimation: Theory and Implementation*. New York, NY, USA: Marcel Dekker, 2004.
[9] M. E. Baran and A. W. Kelley, "A branch-current-based state estimation method for distribution systems," *IEEE Trans. Power Syst.*, vol. 10, no. 1, pp. 483–491, Feb. 1995.
[10] M. E. Baran and A. W. Kelley, "State estimation for real-time monitoring of distribution systems," *IEEE Trans. Power Syst.*, vol. 9, no. 3, pp. 1601–1609, Aug. 1994.
[11] M. Baran, "Branch current based state estimation for distribution system monitoring," in *Proc. IEEE Power Energy Soc. Gen. Meeting*, San Diego, CA, USA, Jul. 2012, pp. 1–4.
[12] W.-M. Lin, J.-H. Teng, and S.-J. Chen, "A highly efficient algorithm in treating current measurements for the branch-current-based distribution state estimation," *IEEE Trans. Power Del.*, vol. 16, no. 3, pp. 433–439, Jul. 2001.
[13] V. Zamani and M. Baran, "Topology processing in distribution systems by branch current based state estimation," in *Proc. North Amer. Power Symp. (NAPS)*, Charlotte, NC, USA, Oct. 2015, pp. 1–5.
[14] M. Ghofrani, M. Hassanzadeh, M. Etezadi-Amoli, and M. S. Fadali, "Smart meter based short-term load forecasting for residential customers," in *Proc. North Amer. Power Symp.*, Boston, MA, USA, Aug. 2011, pp. 1–5.
[15] A. Alimardani, F. Therrien, D. Atanackovic, J. Jatskevich, and E. Vaahedi, "Distribution system state estimation based on nonsynchronized smart meters," *IEEE Trans. Smart Grid*, vol. 6, no. 6, pp. 2919–2928, Nov. 2015.
[16] M. Huang, Z. Wei, G. Sun, and H. Zang, "Hybrid state estimation for distribution systems with AMI and SCADA measurements," *IEEE Access*, vol. 7, pp. 120350–120359, 2019.
[17] C. Tu, X. He, X. Liu, and P. Li, "Cyber-attacks in PMU-based power network and countermeasures," *IEEE Access*, vol. 6, pp. 65594–65603, 2018.
[18] *MicroPMU Datasheet*. Accessed: 2014. [Online]. Available: https://www.pqube3.com
[19] *Guide to the Expression of Uncertainty in Measurement*, Standard ISO-IEC-OIML-BIPM, 1992.
[20] S. Chakrabarti and E. Kyriakides, "PMU measurement uncertainty considerations in WLS state estimation," *IEEE Trans. Power Syst.*, vol. 24, no. 2, pp. 1062–1071, May 2009.
[21] B. P. Hayes, J. K. Gruber, and M. Prodanovic, "A closed-loop state estimation tool for MV network monitoring and operation," *IEEE Trans. Smart Grid*, vol. 6, no. 4, pp. 2116–2125, Jul. 2015.
[22] F. Therrien, I. Kocar, and J. Jatskevich, "A unified distribution system state estimator using the concept of augmented matrices," *IEEE Trans. Power Syst.*, vol. 28, no. 3, pp. 3390–3400, Aug. 2013.
[23] A. Gomez-Exposito, C. Gomez-Quiles, and I. Dzafic, "State estimation in two time scales for smart distribution systems," *IEEE Trans. Smart Grid*, vol. 6, no. 1, pp. 421–430, Jan. 2015.
[24] J. B. Leite and J. R. S. Mantovani, "Distribution system state estimation using the Hamiltonian cycle theory," *IEEE Trans. Smart Grid*, vol. 7, no. 1, pp. 366–375, Jan. 2016.
[25] X. Feng, F. Yang, and W. Peterson, "A practical multi-phase distribution state estimation solution incorporating smart meter and sensor data," in *Proc. IEEE Power Energy Soc. Gen. Meeting*, San Diego, CA, USA, Jul. 2012, pp. 1–6.
[26] K. Samarakoon, J. Wu, J. Ekanayake, and N. Jenkins, "Use of delayed smart meter measurements for distribution state estimation," in *Proc. IEEE Power Energy Soc. Gen. Meeting*, Detroit, MI, USA, Jul. 2011, pp. 1–6.
[27] U. Singh, V. Zamani, and M. Baran, "On-line load estimation for distribution automation using AMI data," in *Proc. IEEE Power Energy Soc. Gen. Meeting (PESGM)*, Boston, MA, USA, Jul. 2016, pp. 1–5.
[28] X. He, X. Liu, and P. Li, "Coordinated false data injection attacks in AGC system and its countermeasure," *IEEE Access*, vol. 8, pp. 194640–194651, 2020.
[29] W. H. Kersting, "Radial distribution test feeders," in *Proc. IEEE Power Eng. Soc. Winter Meeting. Conf.*, Columbus, OH, USA, Aug. 2001, pp. 908–912.
[30] H. Wang, W. Zhang, and Y. Liu, "A robust measurement placement method for active distribution system state estimation considering network reconfiguration," *IEEE Trans. Smart Grid*, vol. 9, no. 3, pp. 2108–2117, May 2018.
[31] A. L. Langner and E. M. Lourenco, "Incorporation of synchronized phasor measurements in generalized state estimation," in *Proc. 12th IEEE Int. Conf. Ind. Appl. (INDUSCON)*, Nov. 2016, pp. 1–6.
[32] M. A. Mohamed, A. S. Al-Sumaiti, M. Krid, E. M. Awwad, and A. Kavousi-Fard, "A reliability-oriented fuzzy stochastic framework in automated distribution grids to allocate μ-PMUs," *IEEE Access*, vol. 7, pp. 33393–33404, 2019.

XI HE (Member, IEEE) received the B.S. degree in electrical engineering and automation from Beijing Jiaotong University, Beijing, China, in 2009, the M.S. degree in software engineering from Zhejiang University, in 2011, and the Ph.D. degree in electric engineering from Hunan University, in 2019. He worked with Hangzhou Hikvision Digital Technology Company Ltd., and Schneider Electric, successively. He is currently a Lecturer with the Hunan Institute of Technology, Hengyang, China. His research interests include cyber security in power grid, synchrophasor measurement, and distribution grid automation.

CHANG LI (Member, IEEE) received the B.S. degree from the School of Electrical Engineering and Automation, Guizhou University, Guiyang, China, in 2014, and the M.S. and Ph.D. degrees from Hunan University, Changsha, China. He is currently a Postdoctoral Research Fellow with the Technical University of Denmark (DTU). His current research interests include modular multilevel converter, high-voltage direct current system stability and control, dc microgird operation and control, and model and control of power electronized power systems.

MINGDI DU received the Ph.D. degree in electronic science and technology from the Huazhong University of Science and Technology, Wuhan, China, in 2014. She is currently an Assistant Professor with the Hunan Institute of Technology University, Hengyang. Her current research interests include photoelectric device and optical networks.

HENG DONG received the B.S. and M.S. degrees in electrical engineering from Hunan University, Changsha, China, in 2006 and 2009, respectively. He was an Electrical Engineer with ZTE and Eaton Corporation, Shenzhen, from 2009 to 2014. He is currently a Lecturer with the Hunan Institute of Technology, Hengyang, Hunan. His research interests include power electronics and smart grid.

PENG LI (Senior Member, IEEE) received the B.Sc., M.Sc., and Ph.D. degrees in electrical engineering from the South China University of Technology, Guangzhou, China, in 1993, 1995, and 2002, respectively, and the Ph.D. degree in electrical engineering from the Technical University of Braunschweig, Braunschweig, Germany, in 2004. He is currently a Professor of Engineering with the Southern Power Grid Digital Grid Research Institute, Guangzhou, China. His research interests include microgrids, renewable energy, and data security.